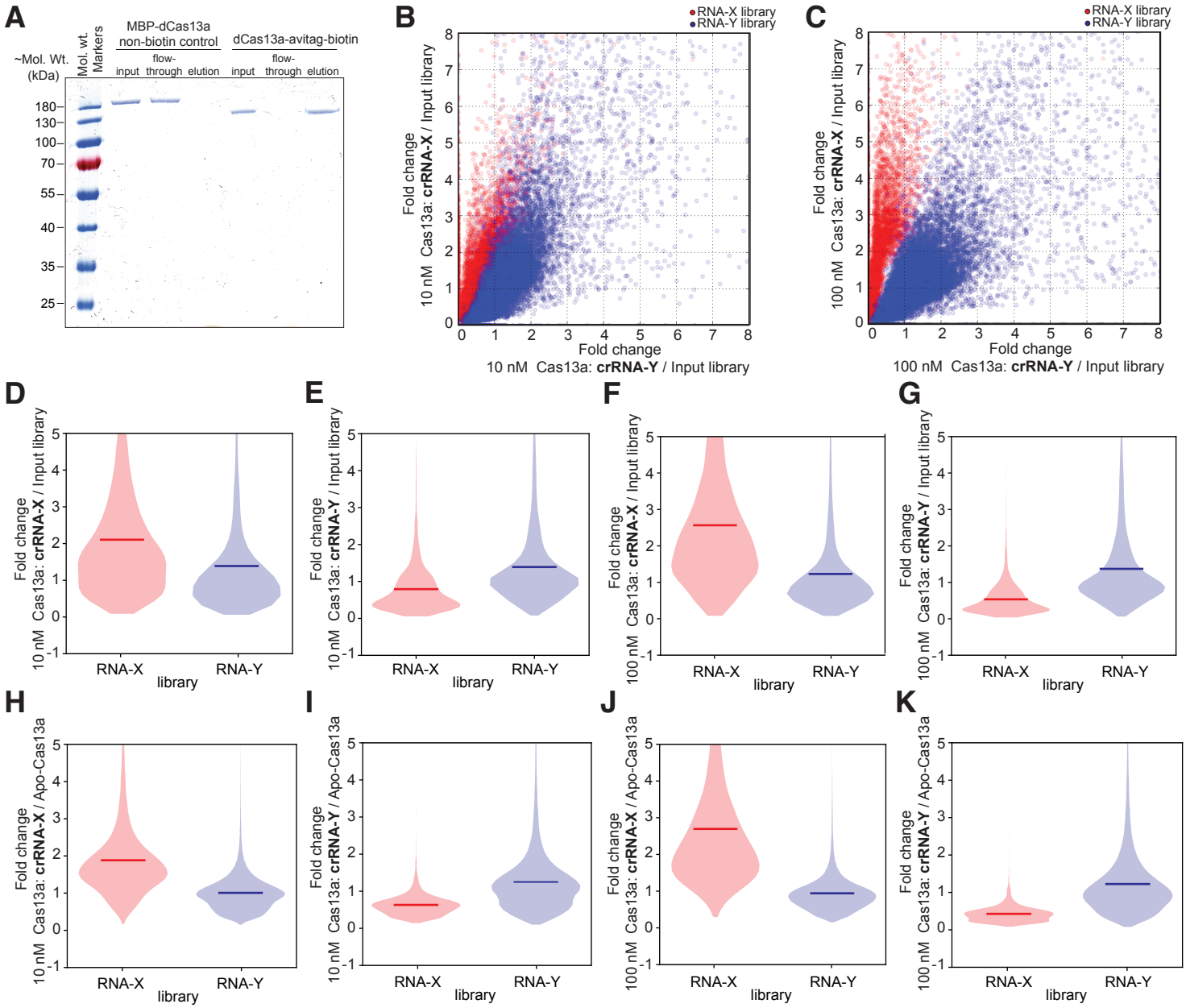

Figure S1: Related to Figure 1. Controls for the development of high-throughput RNA mismatch profiling to determine activator-RNA binding preferences for Lbu-Cas13a. (A) Streptavidin pulldown experiment to confirm Lbu-dCas13a-avitag biotinylation. Streptavidin bead binding assay with biotinylated Lbu-dCas13a-avitag or non-biotinylated MBP-Lbu-Cas13a and streptavidin magnetic beads. 8.5 pmol of biotinylated Lbu-dCas13a-avitag or non-biotinylated MBP-Lbu-Cas13a were separately mixed with 12 µL streptavidin magnetic beads and incubated in modified processing buffer at 37C for 1 h, followed by three washes with modified processing buffer and elution in boiling SDS-PAGE loading buffer.Input, incubation flow-through & elution for each sample were analyzed using SDS-PAGE. Biotinylated Lbu-dCas13a-avitag only remains specifically bound to the beads. (B,C) Scatter plots displaying fold-change in abundance of each RNA-X and –Y library members between samples with (B) 10 nM crRNA-bound Cas13a (vs. input library) or (C) 100 nM crRNA-bound Cas13a (vs. input library) programmed to target RNA-X or -Y ssRNAs. (D-G) Violin plots displaying fold-change in abundance distributions relative to input library for RNA-X and –Y libraries between samples containing (D) 10 nM Cas13a-crRNA-X , (E) 10 nM Cas13a-crRNA-Y, (F) 100 nM Cas13a-crRNA-X and (G) 100 nM Cas13a-crRNA-Y. (H-K) Violin plots displaying fold-change in abundance distributions compared to apo-Cas13a for RNA-X and –Y libraries between samples containing (H) 10 nM Cas13a-crRNA-X , (I) 10 nM Cas13a-crRNA-Y, (J) 100 nM Cas13a-crRNA-X and (K) 100 nM Cas13a-crRNA-Y. The solid line in each plot indicates the sample mean fold-change. Significant crRNA-dependent enrichment (p-value <0.001) of the crRNA-complementary library was observed in all cases using a Welch's 2-tailed t-test.

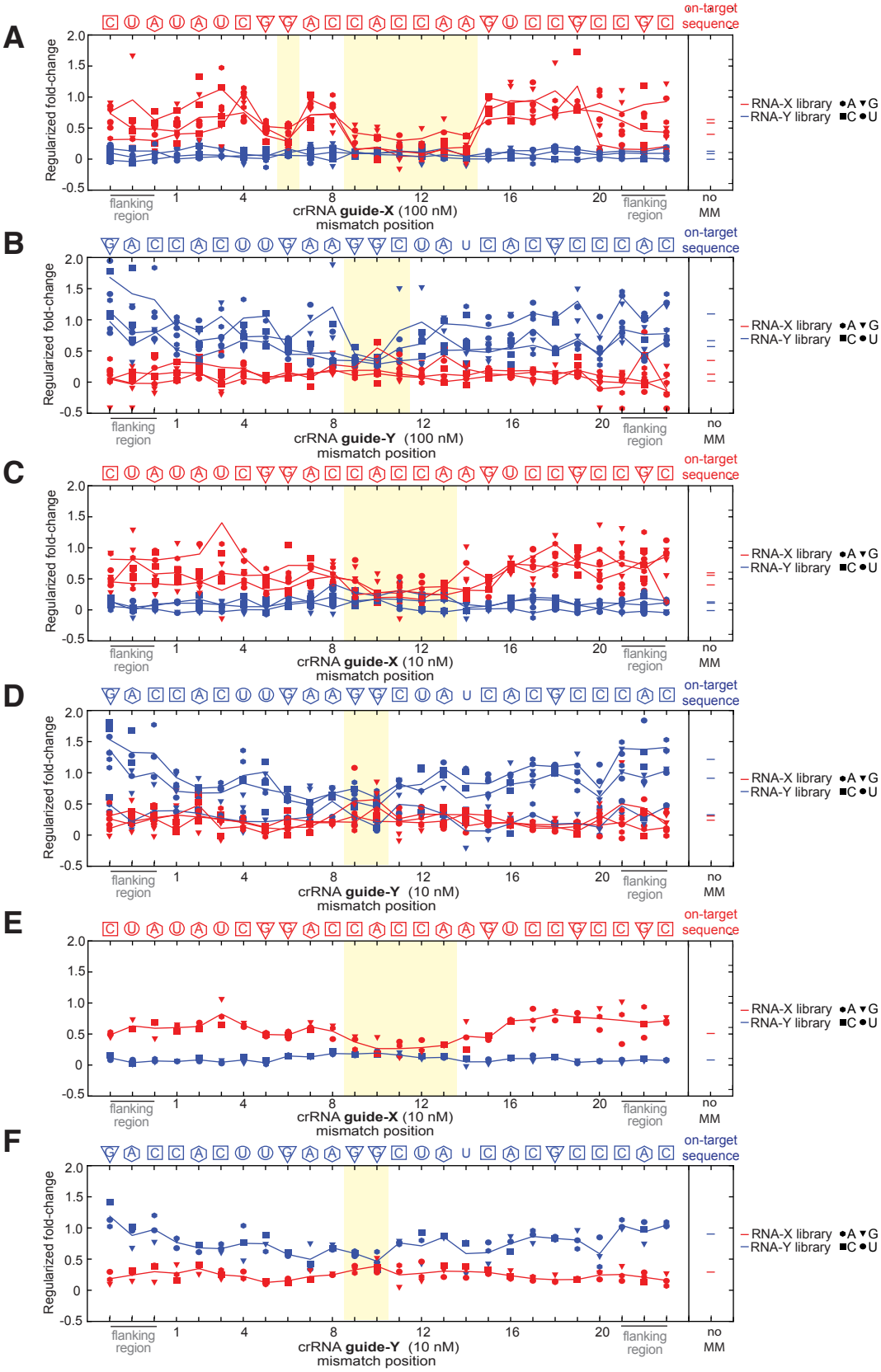

Figure S2: Related to Figure 2. Additional dCas13a high-throughput RNA mismatch profiling data. Regularized fold-change enrichment analysis (relative to Apo-dCas13a) for activator-RNA members of both libraries that contain only a single mismatch across the shown spacer-targeting and flanking regions. Plotting all individual points for (A) targeting X activator-RNA library with 100 nM dCas13a: crRNA-X, (B) targeting Y activator-RNA library with 100 nM dCas13a: crRNA-Y, (C) targeting X activator-RNA library with 10 nM dCas13a: crRNA-X, and (D) targeting Y activator-RNA library with 10 nM dCas13a: crRNA-Y. In each plot, each individual point in a position represents the fold-change value for each unique mismatch combination possible in that position (represented from n=3 experiments), The solid line represents as an average fold-enrichment (of all mismatches combinations) in that position for each experiment. Plotting average points for (E) targeting X activator-RNA library with 10 nM dCas13a: crRNA-X, and (F) targeting Y activator-RNA library with 10 nM dCas13a: crRNA-Y. In each plot, each individual point in a position represents the average regularized fold-change value for each unique mismatch combination possible in that position (from n=3). The solid line represents as an average fold-enrichment (of all mismatches combinations) in that position. The fold-change enrichment of the perfectly complementary (noMM) targets in each experiment are show on the right of each plot. The crRNAcomplementary on-target library sequence is shown above each plot. Positions shaded in yellow indicate where statistically significant ($p < 0.05$) lack of enrichment between guide-complementary and guide-non-complementary sequences was observed. See Methods for regularization and permutation test procedure.

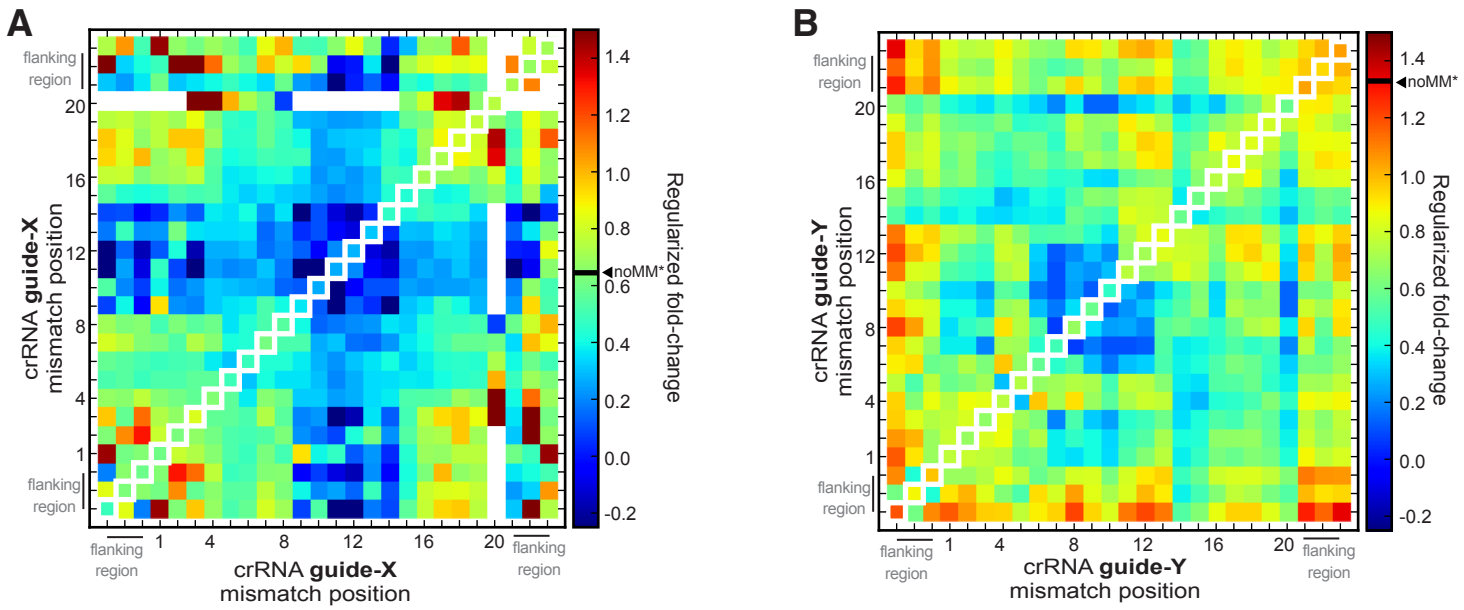

Figure S3: Related to Figure 2. Additional data demonstrating that dCas13a high-throughput RNA mismatch profiling confirms binding mismatch sensitivity hotspots for double-mismatched activator-RNAs. Regularized fold-change enrichment analysis (relative to Apo-dCas13a) for activator-RNA members of both libraries for all pairs of mismatches across the shown spacer-targeting and flanking regions when (A) targeting X activator-RNA library with 10 nM dCas13a: crRNA-X, and (B) targeting Y activator-RNA library with 10 nM dCas13a: crRNA-Y. For comparison, single mismatch data is plotted along the diagonal axis and the fold-change value for a perfectly complementary target is indicated on the heat-map scale bar (noMM*).

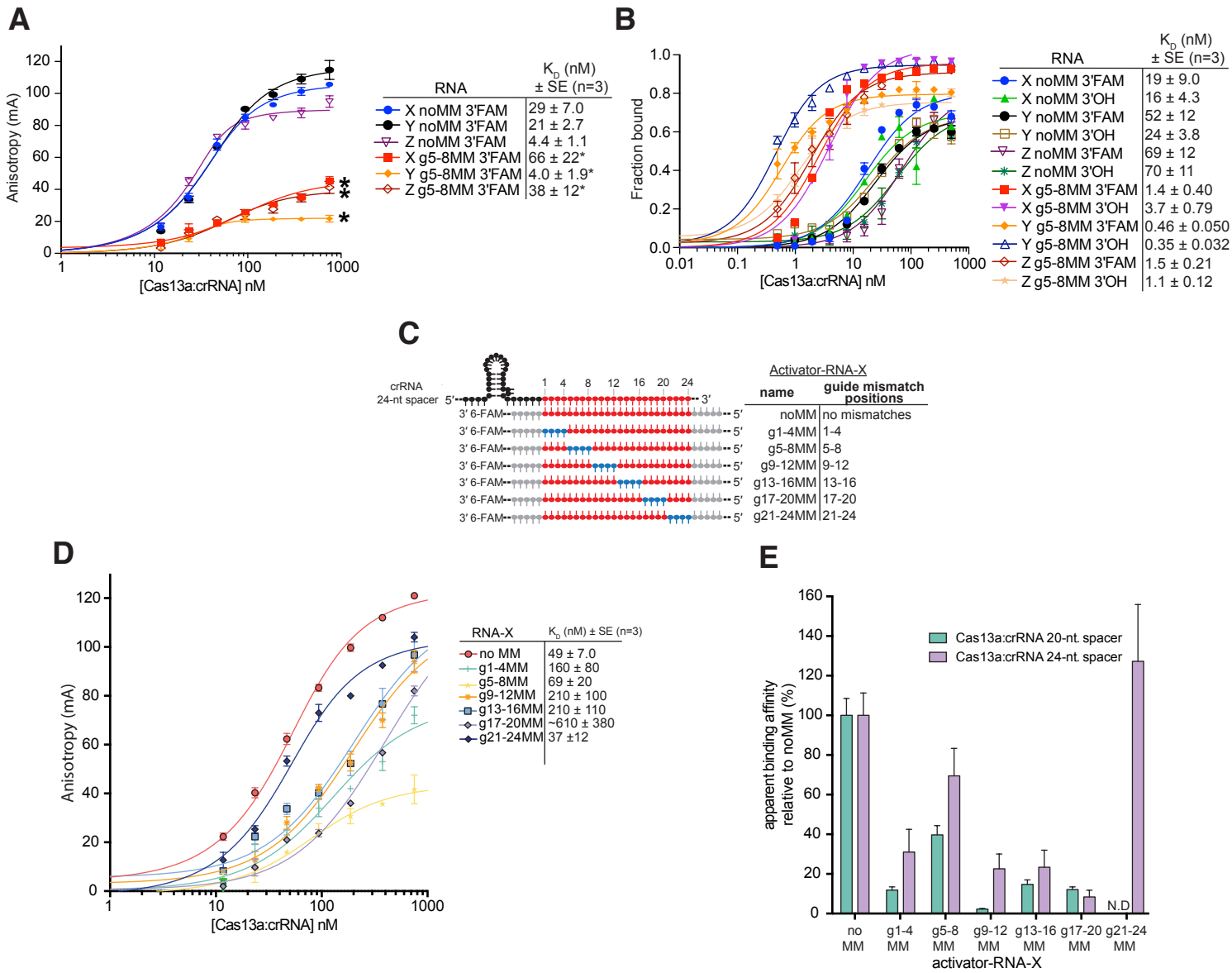

Figure S4: Related to Figure 3 & 4. Additional activator-RNA binding affinity experiments to validate g5-8MM behavior and additional binding affinity experiments using a 24-nt. crRNA-spacer. (A) Fluorescence anisotropy binding curves for the interaction between Lbu-dCas13a: crRNA (sequences X, Y or Z) and activator-RNAs (sequences X, Y or Z) with noMM or g5-8MM mismatches. 3'FAM: 3'-end is modified with a 6-FAM fluorophore. Binding data fits (see Methods) shown as solid lines. Error-bars represent the s.d of the fraction bound from three independent experiments. Dissociation constants (K_D) and their associated standard errors (SE) from three independent experiments are shown. An asterisk (*) indicates measurements for g5-8MM targets that are very likely inaccurate due to very low change in fluorescent anisotropy between unbound and bound activator RNA species. (B) Filter binding curves for the interaction between Lbu-dCas13a: crRNA (sequences X, Y or Z) and activator-RNAs (sequences X, Y or Z) with noMM or g5-8MM mismatches. Activator-RNAs are all labeled with a 5'-32P, and either possess an unmodified 3'-hydroxyl end (3'-OH) or a 3' end modified with 6-FAM fluorophore (3'FAM), and were detected using phosphor-imaging. Binding data fits (see Methods) shown as solid lines. Error-bars represent the s.d of the fraction bound from three independent experiments. Dissociation constants (K_D) and their associated standard errors (SE) from three independent experiments are shown. (C) Schematic of the Lbu-Cas13a crRNA-24-nt.-spacer: activator-RNA interaction highlighting the different activator-RNAs tested in this study. (D) Fluorescence anisotropy binding curves for the interaction between Lbu-dCas13a: crRNA-X (with a 24-nt. spacer) and X activator-RNAs depicted in (C). Binding data fits (see Methods) shown as solid lines. Error-bars represent the s.d of the anisotropy from three independent experiments. Dissociation constants (K_D) and their associated standard errors (SE) from three independent experiments are shown. (E) Data from (D) normalized as a percentage binding affinity relative to the affinity to a perfectly complementary activator-RNA X (no MM).

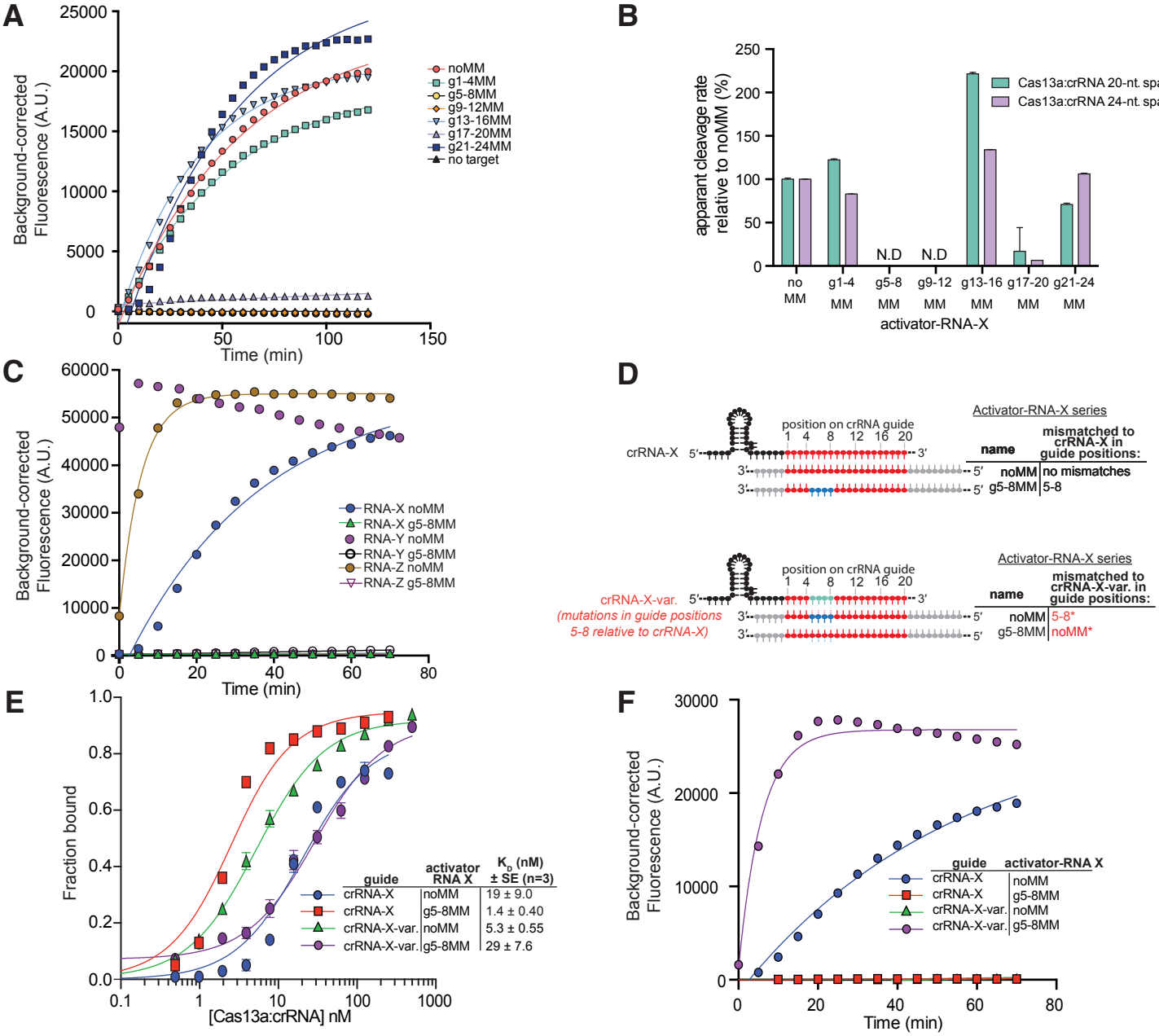

Figure S5: Related to Figure 4. Additional HEPN-nuclease activation experiments with a 24-nt. crRNA-spacer, and additional data showing g5-8MM abolish Lbu-dCas13a HEPN-nuclease activation but not binding. (A) representative time course of background corrected fluorescence measurements generated by Lbu- Cas13a: crRNA-X (with a 24-nt. spacer) activation by the addition of 100 pM activator RNA-X with either zero (noMM) or four consecutive mismatches across the crRNA-spacer region. Quantified data were fitted with single-exponential decays (solid line) with calculated apparent rate constants (k_{obs}) (mean ± s.d., n =3) as follows: noMM 0.025 ± 0.001 min^{-1}, g1-4MM 0.021 ± 0.001 min^{-1}, g13-16MM 0.034 ± 0.001 min^{-1}, g17-20MM 0.002 ± 0.010 min^{-1}, g21-24MM 0.027 ± 0.003 min^{-1} while g5-8MM and g9-12 were not fit. (B) Data from (A) normalized as a percent cleavage rate relative to a perfectly complementary X activator-RNA (noMM) with error bars representing the normalized s.d from three independent experiments. (C) representative time courses of background corrected fluorescence measurements generated by Lbu-Cas13a activation by the addition of 100 pM activator-RNAs with either zero (noMM) or four consecutive mismatches in positions 5-8 of the crRNA-spacer (g5-8MM). Three different RNA sequences (X, Y & Z) and their corresponding crRNAs were tested. Exponential fits are shown as solid lines, except no fit is shown for RNA-Y noMM, as this reaction when to completion before accurate measurements could be taken. (D) Schematic of the Lbu-Cas13a crRNA: ssRNA activator interaction highlighting the position of the mismatches between noMM and g5-8MM RNAs with standard crRNA-X and crRNA-X-variant (crRNA-X-var.; with mismatches in positions 5-8 of the crRNA). (E) Filter binding curves for the interaction between Lbu-dCas13a: crRNA (X, or X-var.) and activator-RNA-X with noMM or g5-8MM mismatches. Activator-RNAs are all labeled with a 5'-32P, and were detected using phosphor-imaging. Binding data fits (see Methods) shown as solid lines. Error-bars represent the s.d of the fraction bound from three independent experiments. Dissociation constants (K_D) and their associated standard errors (SE) from three independent experiments are shown. (F) representative time courses of background corrected fluorescence measurements generated by crRNA-X std- or crRNA-X-var. loaded Lbu-Cas13a activated by the addition of 100 pM activator- RNA-X noMM or RNA-X g5-8MM. Exponential fits are shown as solid lines.

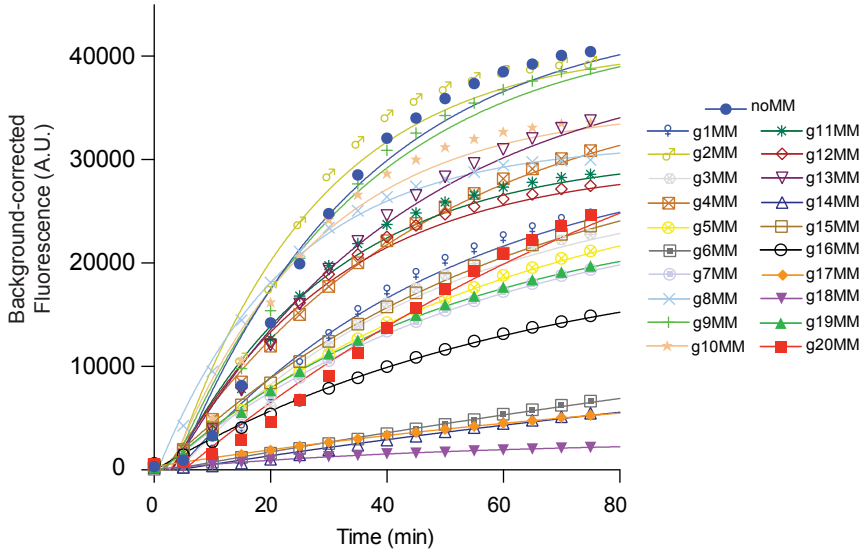

Figure S6: Related to Figure 5. Single mismatch HEPN-nuclease activation time course data. (A) representative time courses of background corrected fluorescence measurements generated by Lbu-Cas13a: crRNA-X activation by the addition of 100 pM activator-RNA-X with either zero or single mismatches within positions 1-20 of crRNA-spacer targeting region (where g1MM= a mismatch between crRNA and target at . Exponential fits are shown as solid lines. Quantified data were fitted with single-exponential decays (solid line) with calculated apparent rate constants (k_{obs}) (mean ± s.d., n =3) as follows: noMM 0.031 ± 0.003 min^{-1}, g1MM 0.022 ± 0.002 min^{-1}, g2MM 0.044 ± 0.008 min^{-1}, g3MM 0.018 ± 0.001 min^{-1}, g4MM 0.027 ± 0.002 min^{-1}, g5MM 0.023 ± 0.001 min^{-1}, g6MM 0.0058 ± 0.0002 min^{-1}, g7MM 0.013 ± 0.0005 min^{-1}, g8MM 0.0124 ± 0.0005 min^{-1}, g9MM 0.020 ± 0.001 min^{-1}, g10MM 0.06 ± 0.02 min^{-1}, g11MM 0.043 ± 0.006 min^{-1}, g12MM 0.048 ± 0.008 min^{-1}, g13MM 0.038 ± 0.005 min^{-1}, g14MM 0.017 ± 0.001 min^{-1}, g15MM 0.047 ± 0.007 min^{-1}, g16MM 0.017 ± 0.001 min^{-1}, g17MM 0.009 ± 0.0002 min^{-1}, g18MM 0.018 ± 0.001 min^{-1}, g19MM 0.021 ± 0.001 min^{-1}, g20MM 0.010 ± 0.0003 min^{-1}.

Data Table S1: Related to Figures 1-2, 5b, S1-3. Illumina sequencing statistics for each HT-RBP sample

Condition	Replicate	Sample ID	Total reads	Unique reads	Unique counts RNA-X	Unique counts RNA-Y	Pairwise x	Pairwise y	Pairwise Pearson (R^2)
10nM Cas13a: crRNA-Y	1	sample_1	15625349	11793370	2104587	9688783	sample_1	sample_2	0.997999
	2	sample_2	15931800	11991568	2265699	9725869	sample_1	sample_3	0.998073
	3	sample_3	15150907	11270000	1948216	9321784	sample_2	sample_3	0.998129
100nM Cas13a: crRNA-Y	1	sample_4	15507952	11980887	1790488	10190399	sample_4	sample_5	0.864246
	2	sample_5	16082538	12226500	1438966	10787534	sample_4	sample_6	0.950326
	3	sample_6	21710528	15530314	2584781	12945533	sample_5	sample_6	0.873170
10nM Cas13a: crRNA-X	1	sample_7	13010814	9768026	3261464	6506562	sample_7	sample_8	0.941342
	2	sample_8	14640111	11228335	2550369	8677966	sample_7	sample_9	0.984130
	3	sample_9	15564034	11365145	3767470	7597675	sample_8	sample_9	0.967258
100nM Cas13a: crRNA-X	1	sample_10	17452867	12623557	4497522	8126035	sample_10	sample_11	0.987434
	2	sample_11	18644215	13605710	4803110	8802600	sample_10	sample_12	0.988626
	3	sample_12	16870822	12775716	3728029	9047687	sample_11	sample_12	0.971437
Apo-Cas13a	1	sample_13	20154071	14367708	4121534	10246174	sample_13	sample_14	0.929286
	2	sample_14	16111507	12379557	2406785	9972772	sample_13	sample_15	0.885397
	3	sample_15	25255372	16919256	3899103	13020153	sample_14	sample_15	0.921500
Input	1	sample_16	16737631	12842032	3536839	9305193	sample_16	sample_17	0.996884
	2	sample_17	21413244	15571405	4360460	11210945	sample_16	sample_18	0.994002
	3	sample_18	19043873	14260906	3985978	10274928	sample_17	sample_18	0.993706

Data Table S2: Related to Figures 1-5, S1-S6. Oligonucleotide sequences used in this study

Oligonucleotide ID*	Type	Source**	Description	Sequence (5'-3')#	Used in Figure(s)
MOC-610	crRNA	PCR-HDV	crRNA-X 20-nt. spacer	ggCCACCCCAAAAAUGAAGGGGACUAAAACAAUAGCCUGGUGGUUCAGGCG	1-6, S1-S2, S4-S9.
MOC-619	crRNA	PCR-HDV	crRNA-Y 20-nt. spacer	ggCCACCCCAAAAAUGAAGGGGACUAAAACAGUGAACUUCCGAUAGUGCGG	2-4, S1-S2, S4-S6, S8.
MOC-616	crRNA	PCR-HDV	crRNA-Z 20-nt. spacer	ggCCACCCCAAAAAUGAAGGGGACUAAAACAGUGGUUCAGGCGGCGCAUGC	S2, S8.
MOC-609	crRNA	PCR-HDV	crRNA-X 24-nt. spacer	ggCCACCCCAAAAAUGAAGGGGACUAAAACAAUAGCCUGGUGGUUCAGGCGGCGC	S1, S7.
MOC-638	crRNA	PCR-HDV	crRNA-X variant (g5-8MM) 20-nt. spacer	ggCCACCCCAAAAAUGAAGGGGACUAAAACAAUAGGGACGUGGUUCAGGCG	S8.
MOC-631	activator-RNA	synthetic (IDT)	3' 6-FAM-labelled activator-RNA X no MM	AACCAGCGGCGGCCUGAACCACCAGGCUAUACCAC/36-FAM/	1, 2, S1-S2, S8.
MOC-637	activator-RNA	synthetic (IDT)	3' 6-FAM-labelled activator-RNA X g1-4MM	AACCAGCGGCGGCCUGAACCACCAGGGAUAACCAC/36-FAM/	1, S1-S2.
MOC-636	activator-RNA	synthetic (IDT)	3' 6-FAM-labelled activator-RNA X g5-8MM	AACCAGCGGCGGCCUGAACCACGUCCCUAUACCAC/36-FAM/	1, 2, S1-S2, S8.
MOC-635	activator-RNA	synthetic (IDT)	3' 6-FAM-labelled activator-RNA X g9-12MM	AACCAGCGGCGGCCUGAAGGUGCAGGCUAUACCAC/36-FAM/	1, 2, S1-S2.
MOC-634	activator-RNA	synthetic (IDT)	3' 6-FAM-labelled activator-RNA X g13-16MM	AACCAGCGGCCGCCACUUCCACCAGGCUAUACCAC/36-FAM/	1, S1-S2.
MOC-633	activator-RNA	synthetic (IDT)	3' 6-FAM-labelled activator-RNA X g17-20MM	AACCAGCGGCGCGGUGAACCACCAGGCUAUACCAC/36-FAM/	1, S1-S2.
MOC-632	activator-RNA	synthetic (IDT)	3' 6-FAM-labelled activator-RNA X g21-24MM	AACCACGCGCGGCCUGAACCACCAGGCUAUACCAC/36-FAM/	S1.
MOC-639	activator-RNA	synthetic (IDT)	3' 6-FAM-labelled activator-RNA Y no MM	AACCAACACCCGCACUAUCGGAAGUUCACACCAC/36-FAM/	2, S2.
MOC-641	activator-RNA	synthetic (IDT)	3' 6-FAM-labelled activator-RNA Y g5-8MM	AACCAACACCCGCACUAUCGGUUCAUCACACCAC/36-FAM/	2, S2.
MOC-640	activator-RNA	synthetic (IDT)	3' 6-FAM-labelled activator-RNA Y g9-12MM	AACCAACACCCGCACUAAGCCAAGUUCACACCAC/36-FAM/	2, S2.
MOC-642	activator-RNA	synthetic (IDT)	3' 6-FAM-labelled activator-RNA Z no MM	AACCAUUAAGCAUGCGCCGCCUGAACCACACCAC/36-FAM/	S2.
MOC-644	activator-RNA	synthetic (IDT)	3' 6-FAM-labelled activator-RNA Z g5-8MM	AACCAUUAACAUGGCGCCGCCACUUCCACACCAC/36-FAM/	S2.
MOC-595	activator-RNA	PCR-HDV	activator-RNA X no MM	ggAACCAGCGGCGGCCUGAACCACCAGGCUAUACCAC	5, 6, S2, S7-S9.
MOC-601	activator-RNA	PCR-HDV	activator-RNA X g1-4MM	ggAACCAGCGGCGGCCUGAACCACCAGGGAUAACCAC	5, S7.
MOC-600	activator-RNA	PCR-HDV	activator-RNA X g5-8MM	ggAACCAGCGGCGGCCUGAACCACGUCCCUAUACCAC	5, S2, S7-S8.
MOC-599	activator-RNA	PCR-HDV	activator-RNA X g9-12MM	ggAACCAGCGGCGGCCUGAAGGUGCAGGCUAUACCAC	5, S7.
MOC-598	activator-RNA	PCR-HDV	activator-RNA X g13-16MM	ggAACCAGCGGCCGCCACUUCCACCAGGCUAUACCAC	5, S7.
MOC-597	activator-RNA	PCR-HDV	activator-RNA X g17-20MM	ggAACCAGCGGCGCGGUGAACCACCAGGCUAUACCAC	5, S7.
MOC-596	activator-RNA	PCR-HDV	activator-RNA X g21-24MM	ggAACCACGCGCGGCCUGAACCACCAGGCUAUACCAC	S7.
MOC-669	activator-RNA	PCR-HDV	activator-RNA Y no MM	ggAACCAACACCCGCACUAUCGGAAGUUCACACCAC	S2, S8.
MOC-671	activator-RNA	PCR-HDV	activator-RNA Y g5-8MM	ggAACCAACACCCGCACUAUCGGUUCAUCACACCAC	S2, S8.
MOC-593	activator-RNA library	SS	activator-RNA X library (for illumina sequencing)	ggACGUGUGCUCUUCCGAUCUJAAGCAUGCGCCGGCCUGAACCACCAGGCUAUAUCUGCNNNNNNAGAUCGGAAGAGCGUCGUG	3-4, 6, S4-6, T1.
MOC-594	activator-RNA library	SS	activator-RNA Y library (for illumina sequencing)	ggACGUGUGCUCUUCCGAUCUGGAUUCAACACCCGCACUAUCGGAAGUUCACCAGCCANNNNNNAGAUCGGAAGAGCGUCGUG	3-4, 6, S4-6, T1.
MOC-563	RT primer (DNA)	synthetic (IDT)	custom Illumina P5 primer containing a 13N UMI	AATGATACGGCGACCACCGAGATCTACACNNNNNNNNNNNNNACACTCTTTCCCTACACGACGCTCTTCCGATC*T	3, T1.
MOC-564	library construction primer (DNA)	synthetic (IDT)	P5 end primer	AATGATACGGCGACCACCG	3, T1.
MOC-673	activator-RNA	PCR-HDV	activator-RNA Z no MM	ggAACCAUUAAGCAUGCGCCGCCUGAACCACACCAC	S2, S8.
MOC-675	activator-RNA	PCR-HDV	activator-RNA Z g5-8MM	ggAACCAUUAAGCAUGCGCCGCCACUUCCACACCAC	S2, S8.
MOC-665	activator-RNA	PCR-HDV	activator-RNA X g1MM	ggAACCAGCGGCGGCCUGAACCACCAGGCUAAACCAC	6, S9.
MOC-664	activator-RNA	PCR-HDV	activator-RNA X g2MM	ggAACCAGCGGCGGCCUGAACCACCAGGCUUUACCAC	6, S9.
MOC-663	activator-RNA	PCR-HDV	activator-RNA X g3MM	ggAACCAGCGGCGGCCUGAACCACCAGGCAAUACCAC	6, S9.
MOC-662	activator-RNA	PCR-HDV	activator-RNA X g4MM	ggAACCAGCGGCGGCCUGAACCACCAGGGUAUACCAC	6, S9.
MOC-661	activator-RNA	PCR-HDV	activator-RNA X g5MM	ggAACCAGCGGCGGCCUGAACCACCAGCCUAUACCAC	6, S9.
MOC-660	activator-RNA	PCR-HDV	activator-RNA X g6MM	ggAACCAGCGGCGGCCUGAACCACCACGCUAUACCAC	6, S9.
MOC-659	activator-RNA	PCR-HDV	activator-RNA X g7MM	ggAACCAGCGGCGGCCUGAACCACCUGGCUAUACCAC	6, S9.
MOC-658	activator-RNA	PCR-HDV	activator-RNA X g8MM	ggAACCAGCGGCGGCCUGAACCACGAGGCUAUACCAC	6, S9.
MOC-657	activator-RNA	PCR-HDV	activator-RNA X g9MM	ggAACCAGCGGCGGCCUGAACCAGCAGGCUAUACCAC	6, S9.
MOC-656	activator-RNA	PCR-HDV	activator-RNA X g10MM	ggAACCAGCGGCGGCCUGAACCUCCAGGCUAUACCAC	6, S9.
MOC-655	activator-RNA	PCR-HDV	activator-RNA X g11MM	ggAACCAGCGGCGGCCUGAAGGACCAGGCUAUACCAC	6, S9.
MOC-654	activator-RNA	PCR-HDV	activator-RNA X g12MM	ggAACCAGCGGCGGCCUGAAGCACCAGGCUAUACCAC	6, S9.
MOC-653	activator-RNA	PCR-HDV	activator-RNA X g13MM	ggAACCAGCGGCGGCCUGAUCCACCAGGCUAUACCAC	6, S9.
MOC-652	activator-RNA	PCR-HDV	activator-RNA X g14MM	ggAACCAGCGGCGGCCUGUACCACCAGGCUAUACCAC	6, S9.
MOC-651	activator-RNA	PCR-HDV	activator-RNA X g15MM	ggAACCAGCGGCGGCCUCAACCACCAGGCUAUACCAC	6, S9.
MOC-650	activator-RNA	PCR-HDV	activator-RNA X g16MM	ggAACCAGCGGCGGCCAGAACCACCAGGCUAUACCAC	6, S9.
MOC-649	activator-RNA	PCR-HDV	activator-RNA X g17MM	ggAACCAGCGGCGGCGUGAACCACCAGGCUAUACCAC	6, S9.
MOC-648	activator-RNA	PCR-HDV	activator-RNA X g18MM	ggAACCAGCGGCGGCGGAACCACCAGGCUAUACCAC	6, S9.
MOC-647	activator-RNA	PCR-HDV	activator-RNA X g19MM	ggAACCAGCGGCCCCCUGAACCACCAGGCUAUACCAC	6, S9.
MOC-646	activator-RNA	PCR-HDV	activator-RNA X g20MM	ggAACCAGCGGCGGCCUGAACCACCAGGCUAUACCAC	6, S9.

***Oligonucleotide ID:** An index to facilitate material-sharing requests as well as maintain continuity between separate publications

**** Source abbreviations:** SS – single-stranded DNA oligonucleotide template was used for in-vitro transcription, PCR-HDV – in-vitro transcription template was a PCR product of overlapping oligonucleotides contains a HDV ribozyme template sequence at the 3' end.

#Sequence colors: red- crRNA-spacer or crRNA-target sequences; **blue**- mismatched nucleotides relative to it parent (prefectly complementary) sequence; Black underline: the partially randomized library portion of the sequence (MOC-593 & MOC-594). This sequence was handmixed to contain 76% of the 'parental' nucleotide and 8% of each other nucleotide in each position.